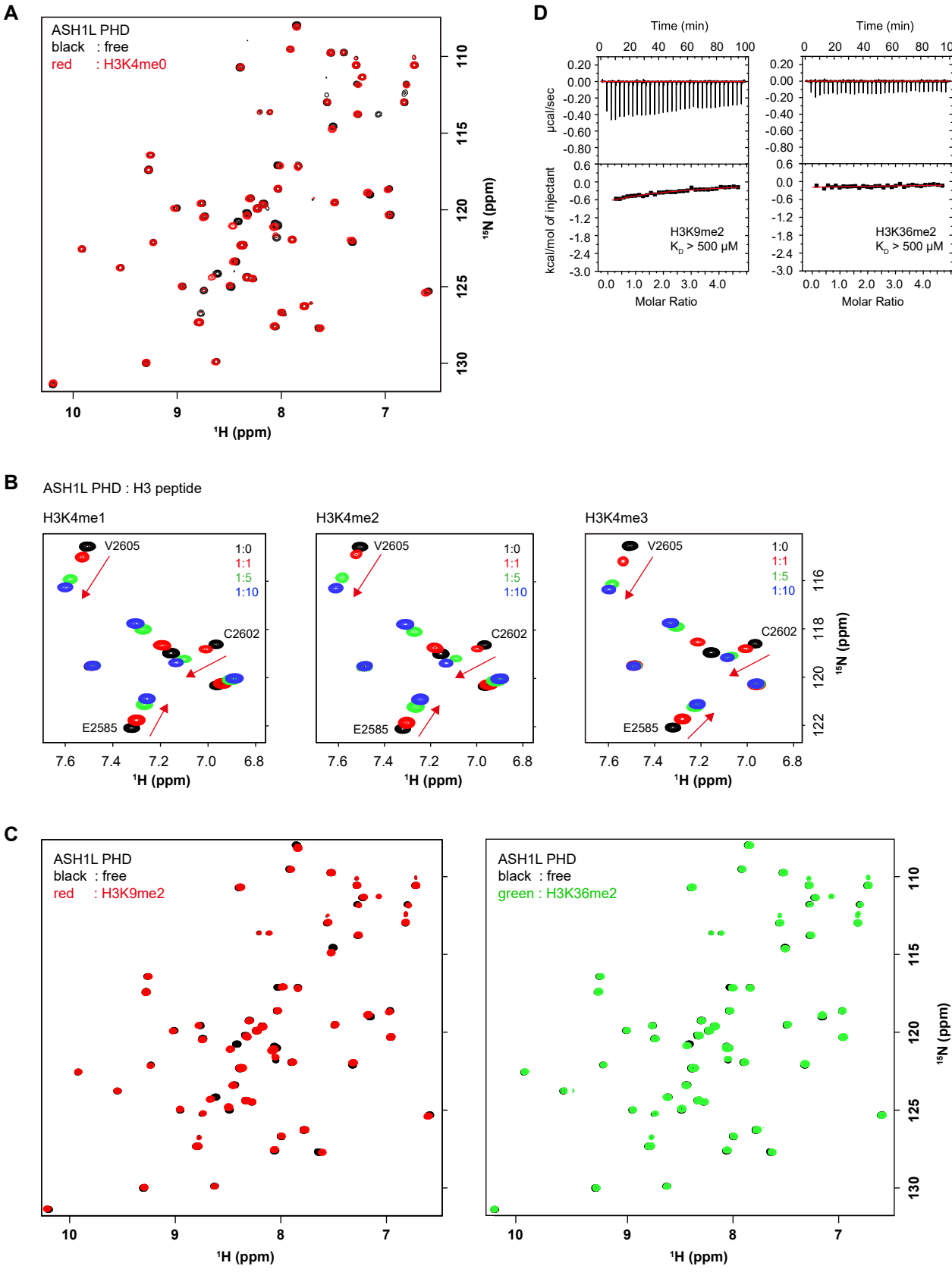


**Supplemental Figure S1**

ASH1L PHD finger binds with methylated H3K4 peptides but not H3K4me0, H3K9me2, or H3K36me2 peptides.

**A**. Superimposed $^{1}$H, $^{15}$N HSQC spectra of ASH1L PHD finger collected without peptide (free) or upon titration with the unlabeled H3K4me0 peptide in a protein: peptide molar ratio of 1: 5.
**B**. Superimposed $^{1}$H, $^{15}$N HSQC spectra of ASH1L PHD finger titrated with indicated peptides. Spectra are color coded according to the ASH1L PHD: peptide molar ratio. Arrows indicate chemical shift changes.
**C**. Superimposed $^{1}$H, $^{15}$N HSQC spectra of ASH1L PHD finger collected without peptide (free) or upon titration with the H3K9me2 or H3K36me2 peptide in a protein: peptide molar ratio of 1: 5.
**D**. Representative binding curves used in $K_D$ determination of H3K9me2 or H3K36me2 peptides with PHD finger by ITC.

**A**

Binding affinity of the ASH1L Bromo-PHD tandem domain

| Peptide H3 (1-15) | $K_D$ (μM) |
|---|---|
| | ITC |
| H3K4 | > 500 |
| H3K4me1 | 64 ± 9 |
| H3K4me2 | 29 ± 3 |
| H3K4me3 | 48 ± 7 |

**B**

ASH1L Bromo-PHD tandem domain
H3 (1-15) peptides

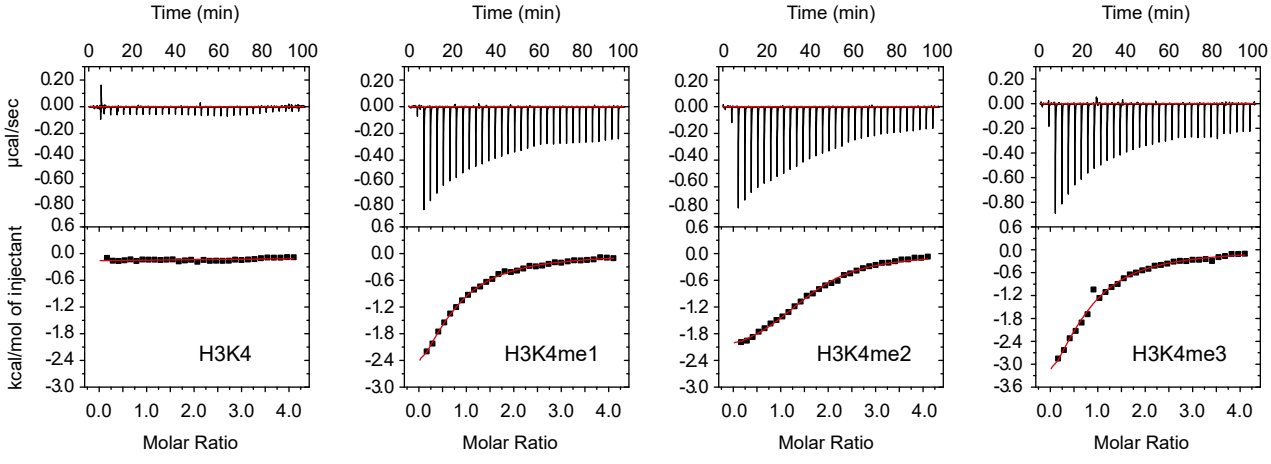


**Supplemental Figure S2**
The binding affinity of ASH1L Bromo-PHD tandem domain (2425-2627 aa) to different methylated H3K4 (1-15) peptides.

**A**. Binding affinity of ASH1L Bromo-PHD tandem domian with indicated H3 (1-15) peptides measured by ITC.
**B**. Representative binding carves used to determine the $K_D$ values in ITC experiments.

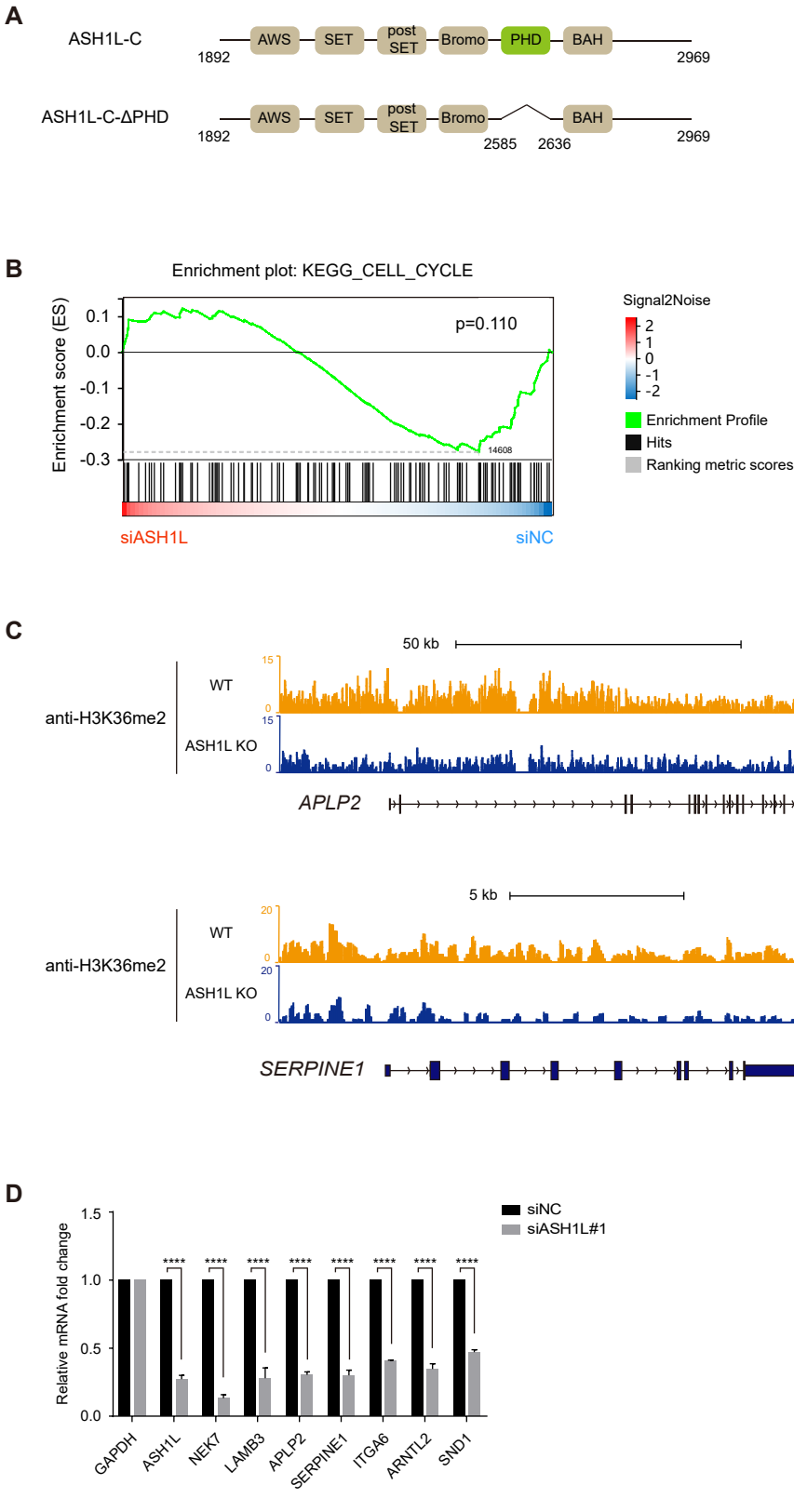


**Supplemental Figure S3**
ASH1L can regulate gene expression by increasing the H3K36me2 level.

**A**. Schematic representation of domains in Flag-ASH1L-C and Flag-ASH1L-C-ΔPHD constructs.
**B**. GSEA of RNA-seq data to analyze the cell cycle pathway altered by ASH1L knockdown in PC3 cells.
**C**. The analysis of available ChIP-seq data (GSE147074) performed in wild type (WT) and ASH1L knockout (KO) BHT-101 cells using H3K36me2 antibody. The H3K36me2 peaks on *APLP2* and *SERPINE1* are decreased after ASH1L knockout.
**D**. qRT-PCR verification of some downregulated genes in PC3 RNA-seq results.

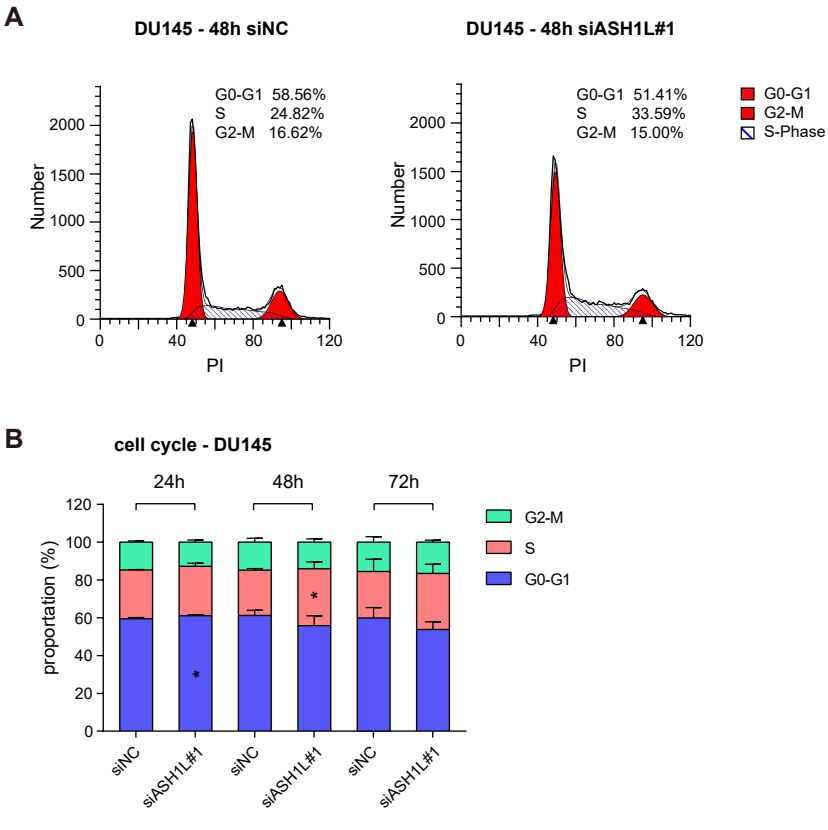


**Supplemental Figure S4**
ASH1L knockdown induced cell-cycle arrest in DU145.

**A**. Representative flow cytometry images about cell cycle distribution of DU145 at 48h after siNC and siASH1L#1 transfection.
**B**. Cell cycle analysis of DU145 at 24, 48, and 72h after siNC and siASH1L#1 transfection.

Supplemental Table S1
Summary of primers for qRT-PCR.

| Gene | Product length | Forward primer | Reverse primer |
|---|---|---|---|
| ASH1L | 75 bp | TCCTTCAAAACGAGACCCTTCA | TCTTCAGACTGGCATTCAATGG |
| GAPDH | 130 bp | GTCTCCTCTGACTTCAACAGCG | ACCACCCTGTTGCTGTAGCCAA |
| CCNA1 | 85 bp | TAGACACCGGCACACTCAAG | AGGAGAGATGAATCTACCAGCAT |
| CCNA2 | 202 bp | GGATGGTAGTTTTGAGTCACCAC | CACGAGGATAGCTCTCATACTGT |
| CCNB1 | 228 bp | AACTTTCGCCTGAGCCTATTTT | TTGGTCTGACTGCTTGCTCTT |
| CCND1 | 195 bp | GCATCTACACCGACAACTCC | CACAGAGGGCAACGAAGGT |
| CCND3 | 173 bp | ACTGGCACTGAAGTGGACTG | ATGGCTGTGACATCTGTAGGAG |
| CDK1 | 148 bp | AAACTACAGGTCAAGTGGTAGCC | TCCTGCATAAGCACATCCTGA |
| CDK2 | 162 bp | AGCCAAGTTTCCCCAAGTG | TGGTCACATCCTGGAAGAAAG |
| CDK4 | 191 bp | GTTCGTGAGGTGGCTTTACTG | ATCGTTTCGGCTGGCAAG |
| CDK6 | 225 bp | GCTGACCAGCAGTACGAATG | GCACACATCAAACAACCTGACC |

Supplemental Table S2
Summary of restraints and statistics of the final 20 structures of ASH1L PHD domain in complex H3K4me2 peptide.

| | PHD/H3K4me2 |
|---|---|
| Protein NMR distance and dihedral constraints | |
| Distance constraints | |
| Total NOE | 1272 |
| Intra-residue | 421 |
| Inter-residue | 851 |
| Sequential (\|i - j\| = 1) | 232 |
| Medium-range ($2 \leq \|i - j\| \leq 5$) | 225 |
| Long-range (\|i - j\| > 5) | 394 |
| Inter-molecular constraints | 62 |
| Hydrogen bonds | 15 |
| Total dihedral angle restraints | |
| Phi angle | 41 |
| Psi angle | 41 |
| Ramachandran Map Analysis (%) | |
| Most favored regions | 94.3 |
| Additional allowed regions | 5.7 |
| Generally allowed regions | 0.0 |
| Disallowed regions | 0.0 |
| Structure statistics | |
| Violations (mean +/- s.d.) | |
| Distance constraints (Å) | 0.063 +/- 0.017 |
| Dihedral angle constraints (º) | 0.45 +/- 0.10 |
| Max. dihedral angle violation (º) | 0.62 |
| Max. distance constraint violation (Å) | 0.092 |
| Deviations from idealized geometry | |
| Bond lengths (Å) | 0.0053 +/- 0.00017 |
| Bond angles (º) | 0.70 +/- 0.033 |
| Impropers (º) | 1.6 +/- 0.090 |
| Average pairwise r.m.s. Deviation ** (Å) | |
| Heavy | 0.73 +/- 0.062 |
| Backbone | 0.25 +/- 0.047 |

**: The residue number ranges used in protein/peptide complex RMSD calculations are 5-52 and 301-305. Pairwise r.m.s. deviation was calculated among 20 refined structures of total 200 structures.
%: Procheck residue numbers are 6-7, 18-24, 26-31, 32-38 and 47-49.

Supplemental Table S3
Summary of binding affinities of different PHD fingers with methylated H3 tail peptides.

| Protein | Peptide | $K_D$ (μM) | Measuring method | Reference |
|---|---|---|---|---|
| PHF20 | H3K4me0 | 73 ± 6 | Tryptophan fluorescence | (1) |
| | H3K4me1 | 49 ± 2 | | |
| | H3K4me2 | 20 ± 6 | | |
| | H3K4me3 | 3.6 ± 0.6 | | |
| MLL5 | H3K4me0 | 778 ± 183 | NMR | (2) |
| | H3K4me1 | 319 ± 18 | | |
| | H3K4me2 | 104 ± 14 | Tryptophan fluorescence | |
| | H3K4me3 | 21 ± 9 | | |
| SET3 | H3K4me0 | 1400 ± 300 | NMR | (3) |
| | H3K4me1 | 790 ± 15 | | |
| | H3K4me2 | 30 ± 5 | Tryptophan fluorescence | |
| | H3K4me3 | 20 ± 7 | | |
| TAF3 | H3K4me3 | 0.31 ± 0.09 | Tryptophan fluorescence | (4) |
| ING2 | H3K4me0 | 2240 ± 350 | NMR | (5) |
| | H3K4me1 | 208 ± 80 | | |
| | H3K4me2 | 15 ± 4 | Tryptophan fluorescence | |
| | H3K4me3 | 1.5 ± 1 | | |
| ING3 | H3K4me0 | 180.62 ± 19.17 | ITC | (6) |
| | H3K4me1 | 23.24 ± 0.80 | | |
| | H3K4me2 | 2.99 ± 0.33 | | |
| | H3K4me3 | 0.93 ± 0.04 | | |

**Reference**


1. Klein BJ, Wang X, Cui G, Yuan C, Botuyan MV, Lin K, et al. PHF20 Readers Link Methylation of Histone H3K4 and p53 with H4K16 Acetylation. Cell reports. 2016;17(4):1158-70. doi: 10.1016/j.celrep.2016.09.056
2. Ali M, Rincón-Arano H, Zhao W, Rothbart SB, Tong Q, Parkhurst SM, et al. Molecular basis for chromatin binding and regulation of MLL5. Proceedings of the National Academy of Sciences of the United States of America. 2013;110(28):11296-301. doi: 10.1073/pnas.1310156110
3. Gatchalian J, Ali M, Andrews FH, Zhang Y, Barrett AS, Kutateladze TG. Structural Insight into Recognition of Methylated Histone H3K4 by Set3. Journal of molecular biology. 2017;429(13):2066-74. doi: 10.1016/j.jmb.2016.09.020
4. van Ingen H, van Schaik FM, Wienk H, Ballering J, Rehmann H, Dechesne AC, et al. Structural insight into the recognition of the H3K4me3 mark by the TFIID subunit TAF3. Structure (London, England : 1993). 2008;16(8):1245-56. doi: 10.1016/j.str.2008.04.015
5. Peña PV, Davrazou F, Shi X, Walter KL, Verkhusha VV, Gozani O, et al. Molecular mechanism of histone H3K4me3 recognition by plant homeodomain of ING2. Nature. 2006;442(7098):100-3. doi: 10.1038/nature04814
6. Kim S, Natesan S, Cornilescu G, Carlson S, Tonelli M, McClurg UL, et al. Mechanism of Histone H3K4me3 Recognition by the Plant Homeodomain of Inhibitor of Growth 3. The Journal of biological chemistry. 2016;291(35):18326-41. doi: 10.1074/jbc.M115.690651